J Solid State Electrochem (2007) 11:939–945
DOI 10.1007/s10008-006-0238-4

ORIGINAL PAPER

Oxygen evolution on aged IrO_x/Ti electrodes in alkaline solutions

E. Guerrini · H. Chen · S. Trasatti

Received: 3 October 2006 / Revised: 20 October 2006 / Accepted: 31 October 2006 / Published online: 1 December 2006

Abstract O_2 evolution from 1 mol dm^{-1} NaOH aqueous solution was studied on IrO_x/Ti electrodes already used for more than 3 years (aged). IrO_x was prepared by thermal decomposition of the chloride in the temperature range from 330 to 500 °C. Half of the electrodes were stored in air between experiments, the other half in water. The state of the electrode surface was monitored by recording voltammetric curves in a potential region prior to O_2 evolution before and after each group of experiments. O_2 evolution was studied by measuring quasistationary current–potential curves. Tafel slopes were derived using two different approaches. The reaction order with respect to OH^- was also determined and found to be fractional. Results show that the reaction mechanism does not depend on either the calcination temperature or the storage conditions. However, stability appears to be higher for electrodes calcined at higher temperatures and stored in air.

Introduction

Oxides of precious metals of the Pt group possess remarkable electrocatalytic properties for a variety of reactions [1]. More specifically, some of them (Ru, Ir, Rh) are among the most active materials for O_2 evolution in acidic solution [2].

IrO_x (nominally IrO_2) can be prepared by thermal decomposition, by anodic electrolytic growth on the parent metal, and by reactive sputtering [3]. The electrolytic oxide is subject to much easier anodic dissolution, while reactive sputtering produces materials of lower surface area. Thus, thermal decomposition of the chloride is the preparation method customarily used [4–6]. There exists consistent evidence that IrO_x is (though little) less active than RuO_x [7], but in compensation, it is anodically much more stable, so much that it can stabilize RuO_x in a mixture against anodic dissolution [8, 9].

Experiments have shown that the activity of these oxides depends on a number of experimental variables [1], including "aging" [10], a variable that is ignored as a rule because kinetic studies are customarily carried out with freshly prepared electrodes. For "aged", we intend electrodes used in laboratory experiments for several years. In a previous study [10], it has been shown that the mechanism of O_2 evolution on IrO_x in acidic solution changes with "aging", electrodes becoming more active with use. This has explained why the reported activity of IrO_x spans a broad range, the Tafel slope varying between values as low as 35 mV and up to 70 mV. Also, a second Tafel slope (>100 mV) appears in the higher current density range, its observation also depending on "aging".

Studies of O_2 evolution in alkaline solution are scanty and definitely less detailed [11, 12]. The main reason is that IrO_x, and especially RuO_x, are not recommended for practical use at high pH because of enhanced anodic dissolution [13]. Nevertheless, O_2 evolution on RuO_x has been systematically investigated as a function of pH [14]. Therefore, in this work, we have studied the kinetics of O_2

Dedicated to Professor Algirdas Vaškelis on the occasion of his 70th birthday.

E. Guerrini · H. Chen · S. Trasatti (✉)
Department of Physical Chemistry and Electrochemistry,
University of Milan,
Via Venezian 21,
20133 Milan, Italy
e-mail: sergio.trasatti@unimi.it

H. Chen
Fujian Institute of Research from the Structure of Matter,
Chinese Academy of Sciences,
Fuzhou, Fujian, People's Republic of China

evolution in alkaline solution on IrO_x electrodes as a function of "aging", thus filling two gaps at the same time.

Experimental

IrO_x was prepared by thermal decomposition of hydrated $IrCl_3$ in the temperature range from 330 to 500 °C, as described previously [15]. The electrodes used in the present work were not freshly prepared, but they had already been subjected to extensive cathodic and anodic investigations, both in acidic and in alkaline solutions for more than 4 years. During their whole life, the electrodes were split into two sets: between experiments, one was permanently stored in pure water, while the other was currently kept in the laboratory air. As put forward previously [10], the idea was to observe the influence of the degree of macroscopic wetting on the electrocatalytic performances.

Electrodes were prepared at 330, 360, 400, 450, and 500 °C. Two electrodes were prepared at each temperature (one stored in water, the other in air). A total of 10 electrodes were prepared.

All experiments were carried out in 1 mol dm^{-3} NaOH aqueous solution using Milli-Q Millipore water and Fluka reagents (purum p.a.). Unless otherwise specified, current density was based on the apparent (geometric) surface area. Electrode potentials were read against a saturated calomelan electrode (SCE scale). The state of the electrode surface was monitored between different experiments by recording voltammetric curves at 20 mV s^{-1} in the potential range from −0.65 to 0.35 V (SCE), i.e., ca. 0.4 to 1.4 V (reference hydrogen electrode).

Kinetic experiments were carried out at 25 °C using a model 273A EG&G potentiostat–galvanostat driven by a personal computer. Experiments were started by keeping the electrode potential at 0.25 V for 10 min and an additional 5 min at 0.3 V. The potential was then increased in steps of 10 mV, reading the current at each potential after 1 min. As the current reached about 0.2 A (*ca.* 0.1 A cm^{-2}), the direction of variation of the potential was reversed and the potential decreased in steps of 10 mV reading the current after 1 min down to a potential where the current became cathodic. At this point, the potential was stepped to 0.25 V for 5 min, and finally, the electrical connection was switched off. A second polarization curve was immediately recorded without removing the electrode from the solution. The aim was to study O_2 evolution on a kinetically stabilized electrode surface.

The order of reaction with respect to OH^- was determined by single-point experiments using the following potential sequence: read the open circuit potential, bring the electrode to 0.3 V for 5 min, step the potential to 0.48 V, read the current after 3 min, step back to 0.3 V for 5 min, and finally switch off the connection. The composition of the solution was varied between 0.1 and 1.0 mol dm^{-3} NaOH, keeping the ionic strength constant at 1.0 mol dm^{-3} by means of $NaClO_4$.

Results and discussion

Structural and electrical properties of IrO_x electrodes prepared by thermal decomposition have been reported in previous papers [15, 16] and need not be discussed here again.

Voltammetric charge

The interpretation of voltammetric curves has been discussed in previous papers [1]. In this work, voltammetric curves were recorded between groups of experiments to monitor the state of the electrode surface. The voltammetric charge has been shown to be a relative measure of the active surface area and can thus be useful to separate electronic from geometric effects, as well as to follow any modification in the electrode morphology [17].

Figure 1 shows the dependence of the voltammetric charge q^* on the calcination temperature. The evident maximum around 350 °C indicates that, at lower temperatures, the decomposition of the precursor is not complete, as already observed previously [16]. At $T>350$ °C q^* decreases with increasing T because of crystallization and sintering.

The data in Fig. 1 indicate that the samples stored in water exhibit a higher voltammetric charge, although the difference becomes smaller as T increases. The higher value of q^* is taken as an indication of a higher hydrous character of the oxide. As the calcination temperature increases, it

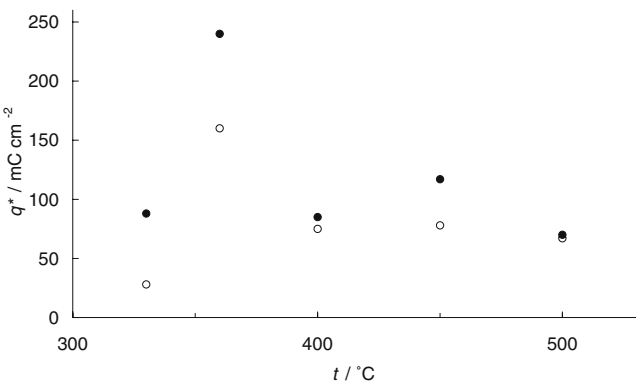

Fig. 1 Voltammetric charge, measured at the beginning of this work in 1 mol dm^{-3} NaOH, as a function of calcination temperature. *Closed circles* electrodes stored in water; *open circles* electrodes stored in air

becomes more difficult to wet the oxygen bridges to form OH groups.

Tafel lines

Figure 2 shows a typical quasistationary current–potential curve. The hysteresis between forward and backward curves and between first and second forward curves is negligible, so much as not to be visible in a drawing.

A linear section is clearly identifiable in Fig. 2, showing that a most likely value of the Tafel slope is 40 mV. This approach to determination of the Tafel slope is here termed "subjective" because the linearization can depend on the operator.

Deviations at higher current densities are attributed to uncompensated ohmic drops, but they can also be related to the existence of a higher Tafel slope. To distinguish between the two possibilities, ΔE values reckoned at constant current in Fig. 2 between experimental points and interpolated straight line are plotted against the relevant current density. Were the deviations in Fig. 2 due only to ohmic drop, a straight line would be observed simulating Ohm's law. Figure 3 shows that this is not the case. The picture is similar for all electrodes. The curvature in Fig. 3 hints to the existence of a higher Tafel slope and higher current densities [18].

An "objective" approach to work out the raw experimental data was used to separate ohmic drops from second Tafel slope effects. The approach, described in previous papers [19], consists in plotting $\Delta E/\Delta j$ reckoned between two experimental points against $(1/j)$, where j is the mean value of current density in the same interval. The outcome for the curve in Fig. 2 is shown in Fig. 4. It is evident that a Tafel slope of 40 mV at low j is followed by a Tafel line close to 120 mV in the high current range, where extrapolation to $(1/j)\rightarrow 0$ gives the average value of the uncompensated resistance (between the electrode surface and the tip of the Luggin capillary) over the explored potential range.

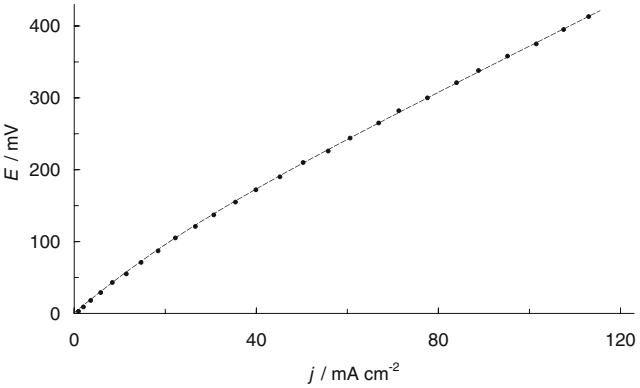

Fig. 3 Typical plot of ΔE (see Fig. 2) as a function of current density from a Tafel line (forward direction) for a IrO_x electrode calcined at 330 °C and stored in air

Tafel slope

Figure 5 shows the Tafel slope as a function of calcination temperature. All electrodes evolve O_2 with the same mechanism involving Tafel slopes close to 40 mV at low overpotentials and close to 120 mV at higher overpotentials. The calcination temperature does not appear to have detectable effects. It is interesting that the "subjective" and the "objective" approaches give the same Tafel slope both forward and backward, while the "subjective" approach cannot allow us, of course, to determine the second Tafel slope, unless very complex calculations are carried out.

The data in Fig. 5 suggest that the way electrodes are stored and the temperature of calcination have no influence on the mechanism of O_2 evolution in alkaline solution.

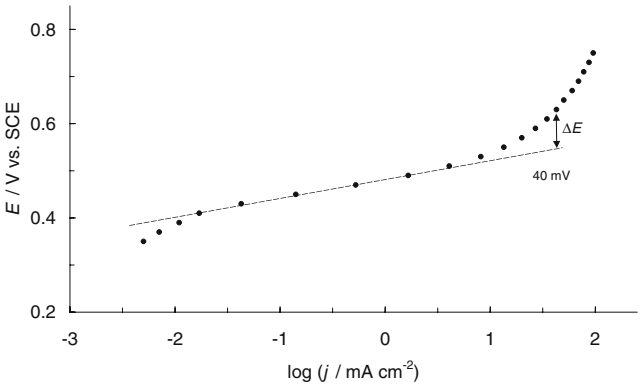

Fig. 2 Typical Tafel line for O_2 evolution in 1 mol dm^{-3} NaOH recorded by increasing overpotential (forward direction). IrO_x electrode calcined at 400 °C and stored in water. *Line* slope of 40 mV dec^{-1} drawn through the raw experimental points

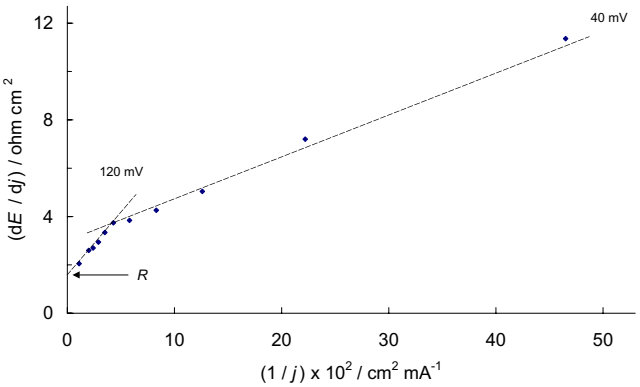

Fig. 4 Typical plot of $\Delta E/\Delta j$ as a function of $1/j$ for an IrO_x electrode calcined at 400 °C and stored in air (data from a Tafel line in the forward direction)

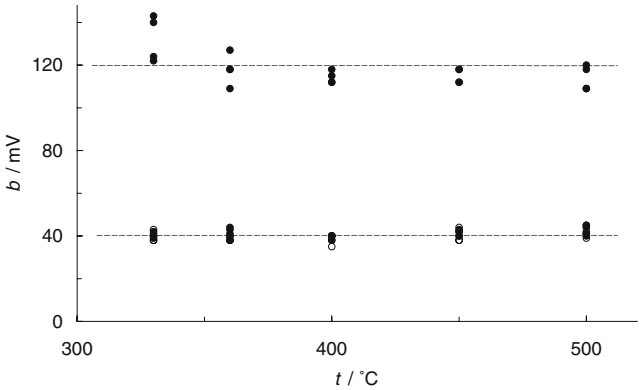

Fig. 5 Tafel slope for O_2 evolution on IrO_x in 1 mol dm^{-3} NaOH as a function of the calcination temperature. *Open circles* electrodes stored in air; *closed circles* electrodes stored in water. Data from forward and backward Tafel lines, for all kinds of electrodes and for both calculation approaches

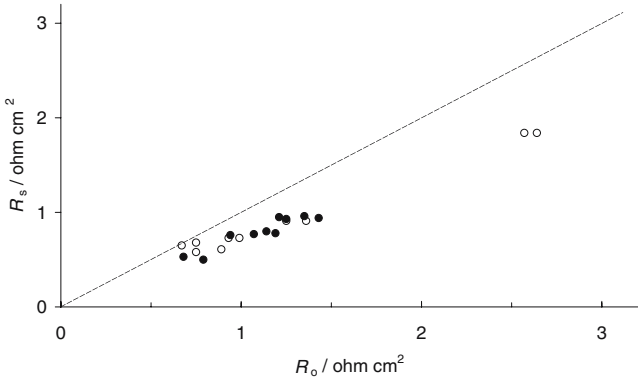

Fig. 7 Uncompensated resistance derived by the "subjective" approach vs uncompensated resistance by the "objective" approach. *Open circles* electrodes stored in air; *closed circles* electrodes stored in water

Uncompensated resistance

Figure 6 shows the dependence of the uncompensated resistance on the calcination temperature. These data were obtained by extrapolation from plots like the one in Fig. 4. The average value of R is typical of conductive oxide layers, the difference between electrodes stored in water and electrodes stored in air being confined to the lowest calcination temperature. The electrodes stored in air exhibit higher ohmic resistance. Because at that temperature the layer is incompletely decomposed and, therefore, not very compact, it is thought that storage in air may result in some growth of an oxide interlayer between Ti and IrO_x.

The difference between the "objective" and the "subjective" approach to work out Tafel lines is evident in Fig. 7. Sometimes, apparent ohmic drops are estimated from the linear portion of curves, such as the one in Fig. 3. Using this approach, apparent ohmic drops are plotted in Fig. 7 against the actual ohmic drops. It is evident that linearization of the data in Fig. 3 tends to underestimate actual ohmic drops, thus leading to incorrect analysis of kinetic data.

Reaction order

Figure 8 shows a typical plot of log j vs log c_{OH^-} for the determination of the reaction order. The way electrodes were stored has no apparent effect on the reaction order.

The dashed straight line drawn through the points has a slope of 1.5 and appears to fit the experimental data closely. Fractional reaction orders are a feature of oxide electrodes [20] and are a consequence of surface charge depending on solution pH [21]. In other words, the reaction order is distorted by double layer effects.

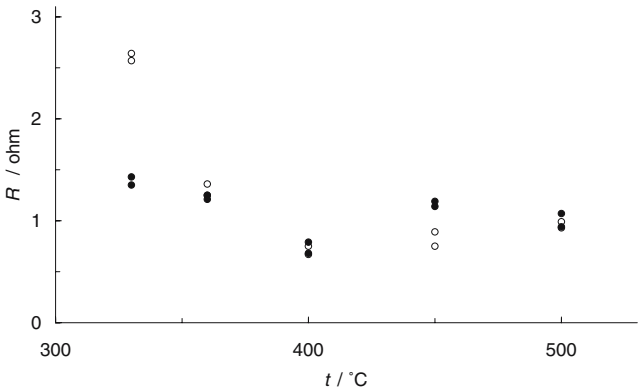

Fig. 6 Uncompensated resistance as a function of calcination temperature. *Open circles* electrodes stored in air; *closed circles* electrodes stored in water. Data from plots such as the one in Fig. 4

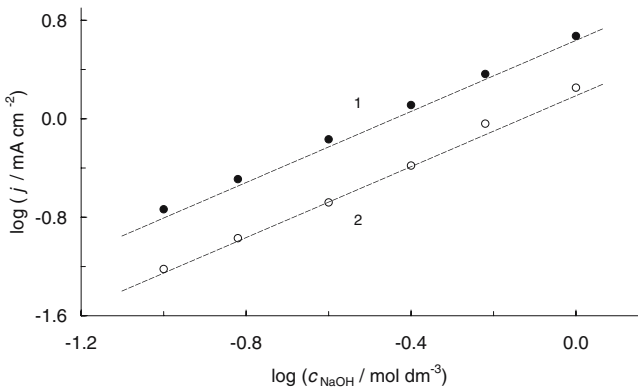

Fig. 8 Typical plot to determine the reaction order of O_2 evolution with respect to OH^-. Current density at 0.48 V (SCE). IrO_x calcined at 450 °C and stored in air (*open circles*) or in water (*closed circles*). *Line* straight line of slope 1.5

Figure 9 shows that the reaction order is closely 1.5 irrespective of the calcination temperature. This indicates that the reaction mechanism does not change with the value of the voltammetric charge, i.e., with the morphology of the electrodes.

Reaction mechanism

The kinetic parameters are unambiguous. For any calcination temperature, and irrespective of the storing conditions, a Tafel slope of 40 mV at lower overpotentials is followed by a higher slope close to 120 mV in the higher overpotentials range. In the low-Tafel-slope region, the order of reaction with respect to OH^- is close to 1.5. The above parameters conform to a classical EE mechanism, the second electron transfer being rate-determined:

$$S + OH^- \rightarrow SOH + e \quad (1)$$

$$SOH + OH^- \rightarrow SO + H_2O + e \quad (2)$$

$$S - O + S - O \rightarrow 2S + O_2 \quad (3)$$

S is a surface-active site. An EE mechanism with $\vartheta_i \approx 0$ predicts a Tafel slope of 40 mV. ϑ_i is the surface coverage with intermediates.

The second Tafel slope of 120 mV is attributed to a transition of the rate-determining step from Eqs. 2 to 1. Such a transition is a rule sharp, which is supported by the data in Fig. 4. Should the transition be due to a mechanism EE with ϑ_i growing from ≈0 to ≈1, a nonlinear region would be observed between the two Tafel lines.

A fractional reaction order has been observed in previous studies with oxides [10, 22] and has been shown to be a manifestation of the surface acid–base equilibrium that these materials establish with protonated solutions [23]. As already demonstrated elsewhere, the value of the apparent reaction order depends on the value of the apparent transfer coefficient [24]. In accord with the mechanism above, the chemically significant reaction order is −2 and the rds is step 2. However, at high pH values, oxide surfaces are negatively charged [21]. Therefore, the electric potential at the reacting site is related to the local concentration of OH^- by the relationship:

$$\phi^* \propto -\frac{RT}{F} \ln c_{NaOH} \text{ or } \phi^* \propto -\frac{RT}{F} \text{pH} \quad (4)$$

In case step 2 above is rate-determining, the reaction rate is given by:

$$j = [SOH][OH^-]\exp[\alpha F(E - \phi^*)/RT] \quad (5)$$

Because step 1 can be assumed to be at quasiequilibrium, and in view of Eq. 4, the following equation results:

$$\ln j \propto (1 + \alpha)\text{pH} + \left[\frac{(1 + \alpha)FE}{RT}\right] \quad (6)$$

It shows that (with $\alpha \approx 0.5$) a reaction order of 1.5 is expected with respect to pH, as observed experimentally.

Structure–activity relation

The surface structure of the oxide electrodes was monitored by measuring the voltammetric charge after groups of experiments. Therefore, a plot of the current density at constant potential for the reaction of O_2 evolution as a function of q^* represents a structure–activity relation [25].

Figure 10 shows the structure–activity relation for O_2 evolution during the forward polarization curve. Thus, the values of q^* are those determined *before* recording Tafel lines. It is intriguing that j and q^* increase monotonically, but not linearly. If q^* is taken as a measure of the surface area, the plot in Fig. 10 suggests that the increase in activity is not only related to geometric (surface area) effects, but also to electronic (catalytic) effects. The latter do not produce a change in the overall mechanism but indicate that

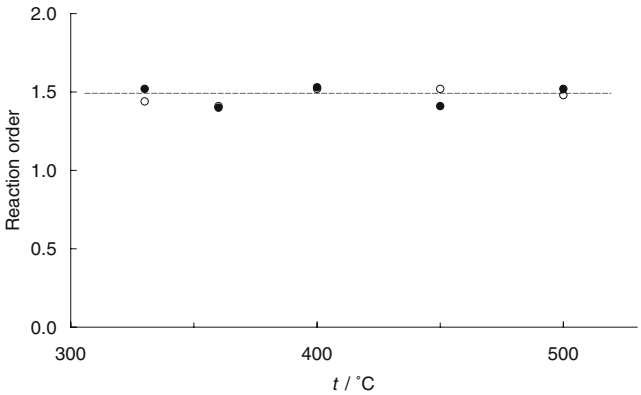

Fig. 9 Reaction order for O_2 evolution on IrO_x as a function of calcination temperature. Electrodes stored in air (*open circles*) and in water (*closed circles*) are distinguished

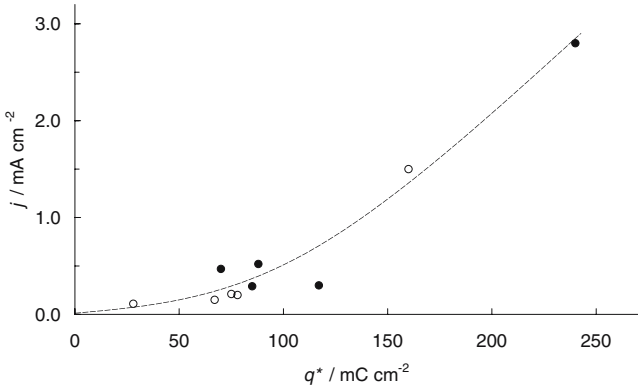

Fig. 10 Activity (j) vs structure (q^*) correlation for O_2 evolution on IrO_x. Voltammetric charge measured at the beginning of this work. Current density at 0.45 V (SCE)

the active sites increase their catalytic properties as q^* increases, i.e., particle size decreases. The increment in activity can be related to edge effects.

IrO_x surfaces are not completely stable under O_2 evolution in alkaline solution, and this is proved by some decrease in q^*. Figure 11 shows a plot of j vs q^*, where currents are taken from the backward polarization curve, and q^* are those determined *after* recording Tafel lines. Curve 1 gathers the electrodes stored in air. Although a small decrease of q^* can be observed with respect to Fig. 10, the pattern of the curve is still the same. The picture is puzzling for the electrodes stored in water. A tentative curve hints to a decrease of activity as q^* increases. In fact, the situation should be looked at from a different point of view. While the electrodes calcined at ≥400 °C show a small decrease in q^*, those calcined at <400 °C show a dramatic drop of q^*, especially the electrode prepared at 360 °C (the maximum in Fig. 2). Such a decrease is presumably not due to mechanical erosion; otherwise, the electrode stored in air would show the same effect. Electrodes stored in water are likely to possess a hydrous structure that can be more easily dissolved by an alkaline solution. In fact, electrodes stored in water show higher stability than those stored in air for O_2 evolution in acid solution [10].

There remains the puzzle of the reverse dependence of j on q^*. A high value of j despite a low value of q^* may indicate that oxide dissolution has left on the surface very thin islands of electrocatalyst with high activity but scarcely detected voltammetrically.

After the Tafel lines, the pattern does not change appreciably. Figure 12 shows the structure–activity relation built up with the current density data taken from reaction order measurements, and q^* values determined *after* the determination of the reaction order. The general features of

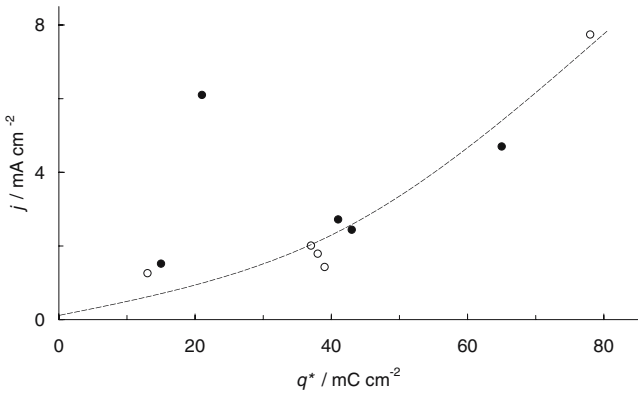

Fig. 12 Activity (j) vs structure (q^*) correlation for O_2 evolution on IrO_x. Current density measured during reaction order determination in 1 mol dm^{-3} NaOH. Voltammetric charge after reaction order determinations. Electrodes stored in air (*open circles*) and in water (*closed circles*) are distinguished

Fig. 10 are retained, although j and q^* values are clearly lower. However, there is still one point that stands up outside the group, corresponding to the electrode calcined at 360 °C and stored in water.

Stability

Because q^* represents the morphology of an oxide electrode, any variation of q^* with use can provide some indication of the stability of the active layer. Figure 13 shows a plot of q^* determined *before* recording the Tafel lines (pristine electrode surfaces for this work, although the electrodes were not virgin, as explained in the introduction) against q^* measured after the reaction order determination (final electrode surfaces for this work). For all electrodes, the plot gives evidence for a marked decrease in q^*, which

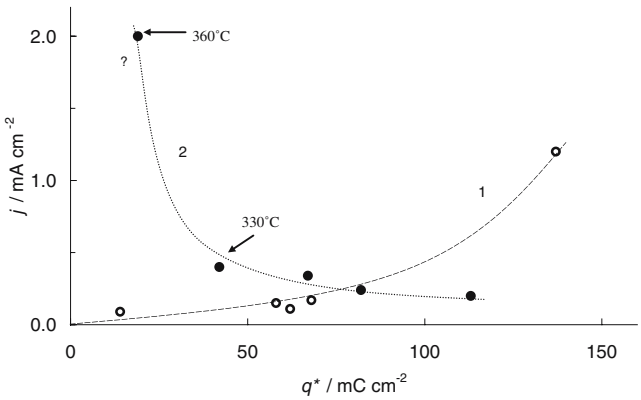

Fig. 11 Same data of activity (j) as in Fig. 10 plotted against the voltammetric charge measured after recording the Tafel lines for O_2 evolution. *1* Apparent correlation for electrodes stored in air (*open circles*); *2* apparent correlation for electrodes stored in water (*closed circles*). The calcination temperature is indicated for two points

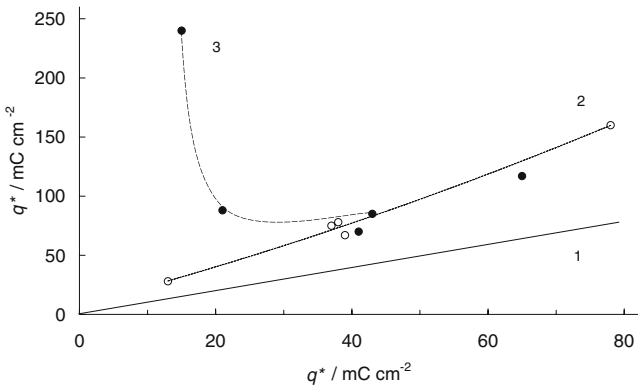

Fig. 13 Initial vs final voltammetric charge of IrO_x in 1 mol dm^{-3} NaOH. *1* Straight line of unit slope (bisect); *2* apparent correlation for electrodes stored in air; *3* apparent correlation for electrodes stored in water

definitely indicates the poor anodic stability under O_2 evolution in alkaline solution. While the correlation is still linear with a positive slope for electrodes stored in air, a reverse dependence is observed for the electrodes stored in water in the region of the low surface charges. These points actually correspond to the electrodes calcined at 330 and 360 °C, respectively.

Conclusions

On aged IrO_x electrodes prepared by thermal decomposition of the chloride, O_2 evolution from alkaline solution occurs with the same mechanism, irrespective of the calcination temperature. The mechanism is also independent of the way IrO_x electrodes are stored when not in use: either in air or in pure water.

Aged IrO_x electrodes are more active than fresh electrodes in the sense that they evolve O_2 with a lower Tafel slope, as already observed also for acidic solutions [10].

Below the calcination temperature of ca. 350 °C, IrO_x electrodes are less stable. The stability is lower for the samples stored in water. IrO_x stored in water exhibit a structure–activity relationship that is not readily understood. This calls for further experimental work aimed at investigating the morphology of IrO_x layers after the dramatic drop in voltammetric charge caused by O_2 evolution on electrodes calcined at <350 °C and stored in water.

Acknowledgement Financial support of Ministero dell'Istruzione, dell'Università e della Ricerca (PRIN) is gratefully acknowledged.

References

1. Trasatti S (1999) In: Wieckowski A (ed) Interfacial electrochemistry. Marcel Dekker, New York, p 769
2. Hrussanova A, Guerrini E, Trasatti S (2004) J Electroanal Chem 564:151
3. Pauportè Th, Andolfatto F, Durand R (1999) Electrochim Acta 45:431
4. de Oliveira-Sousa A, da Silva MAS, Machado SAS, Avaca LA, de Lima-Neto P (2000) Electrochim Acta 45:4467
5. Rossi A, Boodts JFC (2002) J Appl Electrochem 32:735
6. Hu JM, Zhang JQ, Cao CN (2004) Int J Hydrogen Energy 29:791
7. Angelinetta C, Trasatti S, Atanasoska LjD, Minevski ZS, Atanasoski RT (1989) Mater Chem Phys 22:231
8. Kötz R, Stucki S (1986) Electrochim Acta 31:1311
9. Gorodetskii VV, Neburchilov VA, Pecherskii MM (1994) Elektrokhimiya 30:1013
10. Chen H, Trasatti S (1993) J Indian Chem Soc 70:323
11. Miles MH, Huang YH, Srinivasan S (1978) J Electrochem Soc 125:1931
12. Iwakura C, Tada H, Tamura H (1977) J Electrochem Soc Jpn 45:202
13. Buckley DN, Burke LD (1976) J Chem Soc Faraday Trans 1 72:2431
14. Kokoulina DV, Bunakova LV, Eleva MZ (1985) Elektrokhimiya 21:1121
15. Chen H, Trasatti S (1993) J Appl Electrochem 23:559
16. Boodts JFC, Trasatti S (1989) J Appl Electrochem 19:255
17. Trasatti S (1991) Electrochim Acta 36:225
18. Shub DM, Reznik MF (1985) Elektrokhimiya 21:855
19. Krstajić N, Trasatti S (1998) J Appl Electrochem 28:1291
20. Angelinetta C, Falciola M, Trasatti S (1986) J Electroanal Chem 205:347
21. Ardizzone S, Lettieri D, Trasatti S (1983) J Electroanal Chem 146:431
22. Carugati A, Lodi G, Trasatti S (1981) Mater Chem Phys 6:255
23. Krishtalik LI (1981) Electrochim Acta 26:329
24. Trasatti S (1990) In: Wendt H (ed) Electrochemical hydrogen technologies. Elsevier, Amsterdam, p 104
25. Trasatti S (1984) Electrochim Acta 29:1503